PAPER

Check for updates

Synthesis, characterization, and evaluation of selective molecularly imprinted polymers for the fast determination of synthetic cathinones†

Hong Chen,‡[ab] Fangsheng Wu,‡[ab] Yibing Xu,[ab] Yuan Liu,[ab] Lun Song,[ab] Xiujuan Chen,[ab] Qun He,[ab] Wei Liu,[ab] Qiaoying Han,[ab] Zihua Zhang,[ab] Yun Zou*[ab] and Wenbin Liu [ID] *[ab]

As a kind of new psychoactive substance (NPS), synthetic cathinones have drawn great worldwide attention. In this study, molecularly imprinted polymers (MIPs), as adsorbents for the extraction and determination of 4-methyldimethcathinone (4-MDMC), were first synthesized by coprecipitation polymerization. The physicochemical analyses of MIPs were successfully performed by XRD, FTIR, FESEM and TGA techniques. Furthermore, rebinding properties of temperature and pH dependence, and selectivity and reusability tests for MIPs and non-imprinted polymers (NIPs) were performed using an ultraviolet-visible spectrometer (UV-vis). The obtained results indicate that the imprinting efficiency has strong dependence on temperature and pH, and the optimal adsorption for targets is achieved under the condition of 318 K and pH = 6.0. This means that the combination between the polymers and 4-MDMC is a strong spontaneous and endothermic process. Compared with NIPs, MIPs exhibit prominent adsorption capacity (Q_e = 9.77 mg g^{-1}, 318 K). The selectivity coefficients (k) of MIPs for 4-MDMC, methylenedioxypentedrone (βk-MBDP), 4-ethylmethcathinone (4-EMC), methoxetamine (MXE) and tetrahydrofuranylfentanyl (THF-F) were found to be 1.70, 3.49, 7.14 and 5.82, respectively. Moreover, it was found that the adsorption equilibrium was achieved within 30 min. The aim of this work is the simple synthesis of MIPs and the optimal performance of the molecular recognition of 4-MDMC. Moreover, the synthesized MIPs can be easily regenerated and repeatedly used with negligible loss of efficiency (only 9.94% loss after six times adsorption–desorption tests). Satisfying recoveries in the range of 69.3–78.9% indicate that MIPs have good applicability for analyte removal from urine samples. Ultimately, this material shows great promise for the rapid extraction and separation of synthetic cathinones, which are dissolved in the liquid for the field of criminal sciences.

1. Introduction

Over the last few decades, the unprecedented abuse of new psychoactive substances (NPSs) including synthetic cannabinoids, cathinones, phenethylamines and tryptamines is a noticeable phenomenon in the society. Expansion of the illicit drug market poses a great threat to law enforcement and public health protection agencies,[1] while most NPSs are currently defined as illicit substances. According to the official statistics, about 271 million people (5.5% of the global population) worldwide have taken psychoactive drugs at least once during 2019.[2] This is mainly because an increasing number of NPSs are typically given labels such as plant food, bath salts and research chemicals, with similar instructions to "not for human consumption" or "not tested for hazards or toxicity" in order to achieve the ultimate intent of bypassing illegalization.[3,4]

Among these NPSs, synthetic cathinones are notorious for their varieties and hazards, which can produce psychostimulant effects in part attributed to its structure similar to the classically abused agent amphetamine.[5] Until now, more than 140 kinds of synthetic cathinones have been found to contain alkyl or halogen substitutions at points along the aromatic ring as well as methylenedioxy substitutions, pyrrolidinyl substitutions or a combination therein.[6,7] In order to reduce the demand for these cathinones and restrict their commercialization, the determination and identification of illicit drugs in seized samples are very important for integrated public policies. Generally, in forensic drug laboratories, the analytical tools of gas chromatography-mass

Shanghai Key Laboratory of Crime Scene Evidence, Shanghai Research Institute of Criminal Science and Technology, 803 Zhongshan North 1st Road, Shanghai, 200083, P. R. China. E-mail: wbliu1981@163.com; Fax: +86-21-22028361; Tel: +86-21-22028361

Shanghai Yuansi Standard Science and Technology Co., Ltd., 196 Ouyang Road, Shanghai, 200080, P. R. China

† Electronic supplementary information (ESI) available. See DOI: 10.1039/d1ra01330k

‡ These authors contributed equally to this work and should be considered as co-first authors.

spectrometry (GC-MS) and high performance liquid chromatography-mass spectrometry (HPLC-MS) are commonly established to identify and quantify seized drugs and suspicious liquid samples.[8–10] Recently, a number of studies have reported the use of direct analysis in real-time mass spectrometry (DART-MS) that focuses on the characterization of various NPSs.[11] A more convenient detection based on surface-enhanced Raman spectroscopy (SERS) has been reported by Mabbott and his colleagues,[12] and this technique displays an excellent sensitivity for 5,6-methylenedioxy-2-aminoindane and mephedrone. Besides, electrochemistry is an advantageous analytical method that is adaptable to an in-the-field device in light of its portability. In addition, it can exhibit sensitivity and selectivity toward target analytes. Besides, the large majority of relevant reports have used modified electrodes, which are attractive for a preliminary method in forensic analysis.[13–15] Although these methods are known to be reproducible and sensitive for qualitative and quantitative analysis, they suffer from many defects such as high cost, long and complex pre-treatment as well as the need for trained personnel. Therefore, exploiting a facile and versatile method is necessary.

Recently, molecularly imprinted polymers (MIPs) have attracted considerable attention due to their high selectivity, predominant sensitivity, reusability and low cost. Molecular imprinting is known as an efficient technique for the creation of synthetic specific recognition sites in a polymeric network with a memory of the shape, size and functional group of the template molecules.[16,17] With these superior features, MIPs are widely used for applications including sensing,[18] solid phase extraction,[19] antibody detection,[20] separation and purification technology,[21] food analysis[22] and pharmaceutical analysis.[23] The synthesis methods of MIPs are quite simple and mature such as bulk polymerization,[24] precipitation polymerization,[25] membrane polymerization,[26] electro-polymerization,[27,28] multi-step swelling and polymerization and surface-grafting polymerization.[29,30] Precipitation polymerization has been proven very suitable for the synthesis of MIPs because of its mild reaction conditions, simple operation and exemption from additional stabilizers or surfactants.

In this study, we report one-step synthesis of MIPs and its application for the determination of 4-methyl-dimethcathinone (4-MDMC). MIPs were synthesized by a precipitation polymerization method using 4-MDMC as a template, methacrylic acid as a functional monomer and ethylene glycol dimethacrylate as a cross-linker. The chemical structures and physical properties of the obtained MIPs were characterized by a series of experimental techniques such as FT-IR, XRD, TGA and FESEM. The effect of temperature and pH on adsorption was investigated, and the adsorption kinetics and isotherms, selective recognition and regenerative performance of MIPs were systematically elaborated in detail. To the best of our knowledge, this is the first adsorption attempt for the preparation of MIPs to detect synthetic cathinones.

2. Experimental section

2.1 Chemicals and reagents

The chemicals 4-methyldimethcathinone (4-MDMC, $C_{12}H_{17}NO$), methylenedioxypentedrone (βk-MBDP, $C_{13}H_{17}NO_3$), 4-ethylmethcathinone (4-EMC, $C_{12}H_{17}NO$), methoxetamine (MXE, $C_{15}H_{21}NO_2$) and tetrahydrofuranylfentanyl (THF-F, $C_{24}H_{30}N_2O_2$) were supplied by Shanghai Research Institute of Criminal Science and Technology. Methacrylic acid (MAA), 2,2-azobisbutyronitrile (AIBN), ethylene glycol dimethacrylate (EGDMA), absolute ethanol, potassium dihydrogen phosphate (KH_2PO_4), dipotassium hydrogen phosphate (K_2HPO_4), methanol and acetic acid were all purchased from Shanghai Titanchem Co., Ltd. (China). Hydrochloric acid (HCl) and potassium hydroxide (KOH) were bought from Aladdin Reagent Co., Ltd. (China). The above-mentioned chemicals were of analytical grade and used as received without further purification. Methanol of HPLC grade was also acquired from Shanghai Titanchem Co., Ltd. (China). Ultrapure water of 18 MΩ cm^{-1} of resistivity was obtained using a Milli-Q water purification system (Millipore, USA).

2.2 Instruments

The phase compositions of MIPs and NIPs samples were analyzed using powder X-ray diffraction patterns (XRD, Shimadzu, Lab XRD-6000, Japan) with Cu Kα radiation (λ = 0.154 Å). Field emission scanning electron microscopic (FESEM) images were collected using a Nova NanoSEM 450 scanning electron microscope (FEI, USA). Fourier transform infrared (FT-IR) spectroscopy was performed using a Frontier infrared spectrometer (PerkinElmer, USA) over the range of 500–4000 cm^{-1} with KBr pellets. Thermogravimetric analysis (TGA) was carried out from 30 to 800 °C at a heating rate of 10 °C min^{-1} in an atmosphere of nitrogen using a TGA 4000 Thermal Analyzer (PerkinElmer, USA). UV-vis adsorption spectra were recorded using a Lambda 365 spectrometer (PerkinElmer, USA). The real urine samples were tested using an Shimadzu LC-20A HPLC system equipped with a diode array inspection (DAD) system in the experiment.

2.3 Synthesis of molecularly imprinted polymers for 4-MDMC

Molecularly imprinted polymers (MIPs) and non-imprinted polymers (NIPs) were successfully synthesized by a coprecipitation polymerization approach using 4-MDMC as a template. Typical experiments were performed as follows: 0.1 mmol of 4-MDMC and 0.4 mmol of MAA were dissolved in 5 mL of acetonitrile, followed by ultrasonic stirring for 10 min at room temperature to form a homogeneous solution. Subsequently, the mixed solution was magnetically stirred at room temperature for 12 h to obtain the pre-polymerization complex solution. After that, 10 mmol of EGDMA and 10 mg of AIBN were added to the above pre-polymerization complex solution. The solution was deoxygenated with nitrogen for 10 min and magnetically stirred at 70 °C in a water bath for 12 h. The obtained polymers were

eluted with a methanol/acetic acid solution (9 : 1, v/v) to extract the template 4-MDMC and rinsed adequately with methanol and absolute ethanol. Finally, the products were dried in vacuum at 50 °C to a constant weight. Moreover, the NIPs were also prepared under the same condition without the addition of the template. The schematic of the preparation procedure of MIPs is simply shown in Fig. 1.

2.4 Adsorption experiments

To evaluate the adsorption capacity of MIPs and NIPs, static and dynamic adsorption experiments were investigated. In the adsorption thermodynamics experiment, 10 mg of MIPs (or NIPs) was dispersed in a series of 10 mL 4-MDMC solution (10 mmol L^{-1} phosphate buffer solution (PBS), pH = 6.0) with different initial concentrations ranging from 5 to 50 mg L^{-1}. After mechanical shaking for 300 minutes at three different temperatures (298, 308, and 318 K), the MIPs and NIPs were separated by filtering through a 0.22 μm membrane, and the concentrations of the supernatants were further analyzed using a UV-vis spectrometer at 260 nm. The amount of 4-MDMC adsorbed was estimated using the following equation:

$$Q_e = \frac{C_0 - C_e}{m} V \tag{1}$$

where Q_e (mg g^{-1}) represents the equilibrium adsorption capacity, m (mg) the mass of MIPs or NIPs used, V (mL) the volume of the solution, and C_0 (mg L^{-1}) and C_e (mg L^{-1}) the initial and equilibrium concentrations of 4-MDMC, respectively.

In the dynamic adsorption study, 10 mg of MIPs (or NIPs) was suspended in 10 mL of 40 mg L^{-1} 4-MDMC solution (10 mmol L^{-1} PBS, pH = 6.0) and shaken at three different temperatures (298, 308, and 318 K). The real-time concentration of 4-MDMC in the supernatant solutions was also monitored after a series of time intervals from 10 min to 300 min, which was calculated using the following equation:

$$Q_t = \frac{C_0 - C_t}{m} V \tag{2}$$

where Q_t (mg g^{-1}) means the temporal binding capacity of 4-MDMC, and C_0 (mg L^{-1}) and C_t (mg L^{-1}) the initial and temporal 4-MDMC concentrations, respectively. V (mL) is the sample volume, and m (mg) the mass of MIPs or NIPs added to the solutions.

Meanwhile, the influence of solution pH on the adsorption capacity was studied by measuring the binding amounts at different PBS solution pH values (2.0–12.0, adjusted by corresponding 0.1 mol L^{-1} HCl and 0.1 mol L^{-1} NaOH). Besides, selectivity experiments were evaluated towards 40 mg L^{-1} 4-MDMC, 4-EMC, βk-MBDP, MXE and THF-F in 10 mmol L^{-1} PBS (pH = 6.0) solution at 318 K, respectively. The operating sequences and conditions were consistent with the static adsorption tests. After shaken for 300 min, the mixtures were centrifuged and then filtered using a 0.22 μm membrane, and the concentrations of the supernatants were determined using a UV-vis spectrometer. The selectivity and

recognition ability of the MIPs (or NIPs) were evaluated by the selectivity coefficient (k) and imprinting factor (α), respectively, which are defined as follows:

$$K_d = \frac{Q_e}{C_e} \tag{3}$$

$$k = \frac{K_{d(4\text{-MDMC})}}{K_{d(ana)}} \tag{4}$$

$$\alpha = \frac{K_{d(MIPs)}}{K_{d(NIPs)}} \tag{5}$$

where $K_{d(4\text{-MDMC})}$ and $K_{d(ana)}$ (mL g^{-1}) are the partition coefficients of MIPs (or NIPs) toward 4-MDMC and the analogues, Q_e (mg g^{-1}) the equilibrium adsorption capacity and C_0 (mg L^{-1}) and C_e (mg L^{-1}) the initial and equilibrium concentrations of 4-MDMC. $K_{d(MIPs)}$ and $K_{d(NIPs)}$ (mg g^{-1}) refer to the partition coefficients of MIPs and NIPs toward the adsorbed samples, separately.

2.5 Stability and reusability

The stability and reusability of MIPs or NIPs were investigated as follows: 10 mg of MIPs (or NIPs) was added into 10 mL of 4-MDMC solution with a concentration of 40 mg L^{-1} (10 mmol L^{-1} PBS, pH = 6.0) and shaken at 308 K for 300 min. The samples were separated by centrifugation. The recycled MIPs (or NIPs) were washed repeatedly with a mixture of methanol/acetic acid solution (9 : 1, v/v) to remove the template, rinsed with methanol to neutral state and dried in a vacuum. The adsorption–regeneration testing was repeated six times by the above-mentioned method, and the recovery was evaluated according to the following equation:

$$R = \frac{C_i - C_n}{C_i} \times 100\% \tag{6}$$

where R and C_i (mg mL^{-1}) are the recovery and the initial concentration of 4-MDMC (namely 40 mg L^{-1}), respectively. C_n (mg mL^{-1}) is the concentration of 4-MDMC in the supernatant after repeated experiments, and n is the number of times the experiments were repeated (n = 1, 2, 3, 4, 5, and 6).

2.6 Determination of 4-MDMC in human urine

The human urine samples were obtained from laboratory staff volunteers. The urine samples were centrifuged at 5000 rpm for 10 min and the supernatant was filtered using a 0.22 μm membrane for subsequent solid phase extraction. First, 30 mg of MIPs was put into 5.0 mL methanol under continuous stirring for 10 min, which was separated by centrifugation, and the supernatant was discarded. The treated MIPs were dispersed in 5.0 mL 4-MDMC urine samples (40–400 μg L^{-1}) and shaken for 1 h. After the solution was separated by centrifugation and washed with ultrapure water, the analytes were collected from the MIPs, which were rinsed five times with methanol. Finally, the eluent was dried with nitrogen. The residues were redissolved in 200 μL methanol and further analyzed by HPLC at 210 nm.

3. Results and discussion

3.1 Preparation of MIPs

spectra of MIPs, unextracted MIPs and NIPs, where the bands in 2954 cm^{-1}, 1452 cm^{-1} and 1389 cm^{-1} correspond to the stretching vibration of C–H$_3$ and the bending vibration of C–H, –CH$_2$ groups and –CH$_3$ groups, respectively.[34,35] Moreover, the
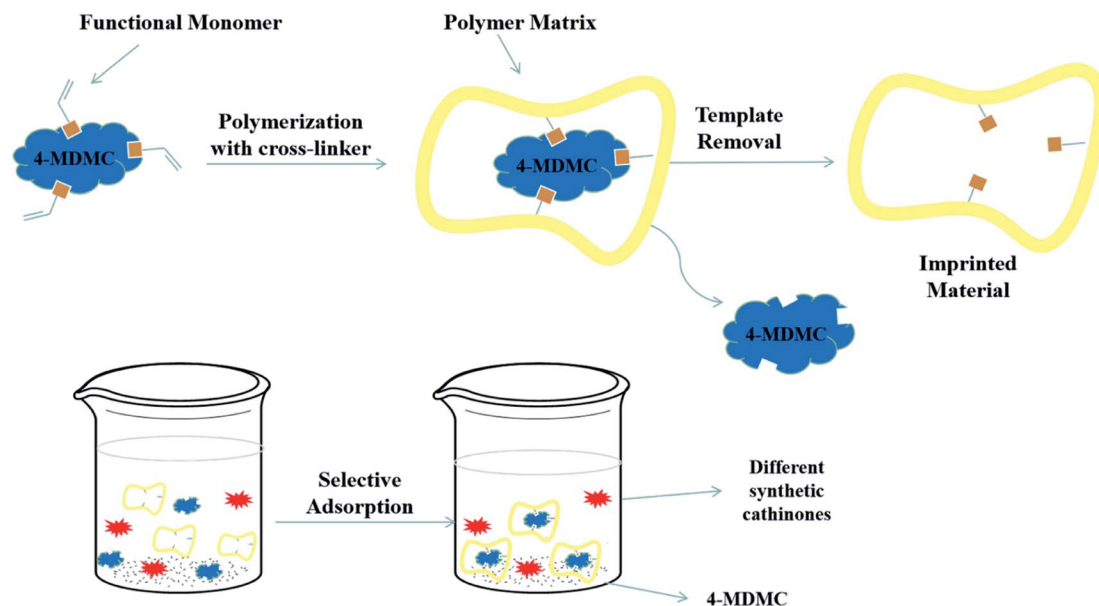

Fig. 1   Schematic of the MIP preparation and application in extraction process and possible recognition mechanism by temperatures.

3.2 Characterization of MIPs and NIPs

The X-ray powder diffraction patterns of MIPs, unextracted MIPs and NIPs are shown in Fig. S1A.† It can be seen that MIPs and unextracted MIPs exhibit a typical similar diffraction profile without any peaks and crystallinity, suggesting that both polymers are amorphous materials.[31] The above characteristics are common for polymers.[32] As for the synthesized NIPs without 4-MDMC as a template, there are no changes in the crystallinity. The above analysis indicates that the 4-MDMC has no significant impact on the crystalline behavior of molecularly imprinted polymers.[33]

FT-IR measurement was used to characterize the samples in the form of KBr pressed pellets. Fig. S1B† shows the FT-IR

characteristic peak at 1144 cm^{-1} is assigned to the C–O–C stretching vibration in monomers and cross-linkers. Generally, the signal ascribed to the C=O bond of the polymers obviously appears at 1719 cm^{-1}.[36] Besides, the characteristic peak at 1640 cm^{-1} refers to the stretching vibration of the C=C bond in alkene. Moreover, the spectra of the MIPs and NIPs are almost the same because the chemical compositions are similar after elution of the template from the MIPs. These results indicate that the template well interacts with the cross-linking functional monomer through hydrogen bonds.[37]

In addition, thermal stabilities about the MIPs, unextracted MIPs and NIPs were studies. As exhibited in Fig. 2A, the TGA curves of the MIPs, unextracted MIPs and NIPs reveal very similar profiles mainly including two stages. In the first step,
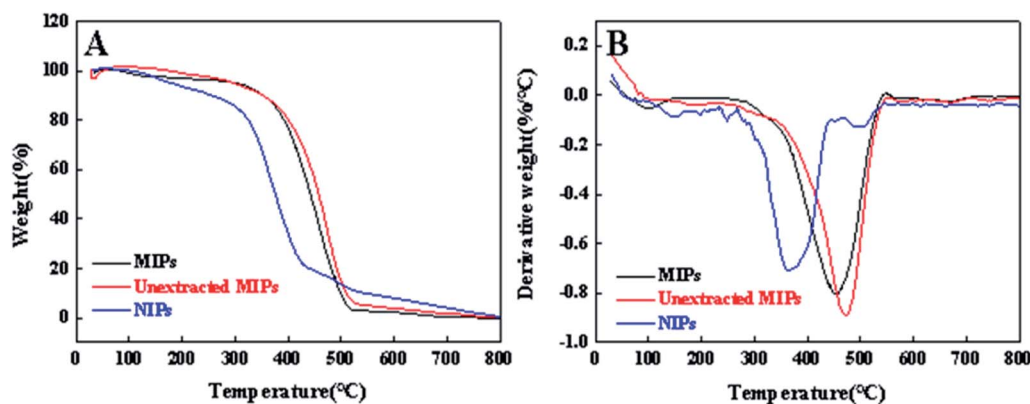

Fig. 2   (A) TGA thermograms and (B) DTG plots of MIPs, unextracted MIPs and NIPs in the range of 30–800 °C.
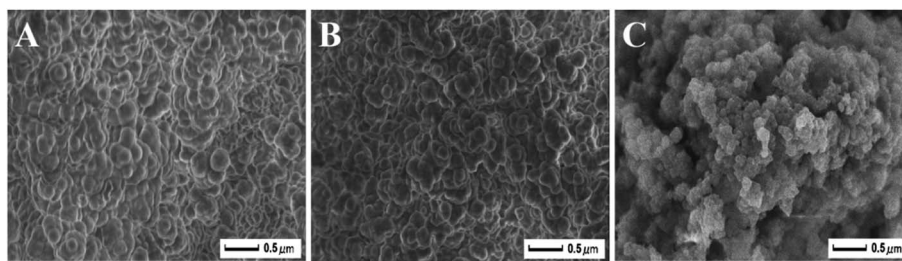
Fig. 3 SEM images (A) MIPs, (B) unextracted MIPs and (C) NIPs.

a slight weight loss at 30–150 °C is attributed to the evaporation of adsorbed water and possible solvents used in the synthesis. The second event of mass loss can be ascribed to the thermal decomposition of the material.[38] However, decomposition of the NIPs starts immediately after melting (~360 °C) in a single ramp, with a total mass loss of 99.4%, and the MIPs and unextracted MIPs occur at a maximum temperature of 452 °C and 473 °C, which is consistent with the results shown in Fig. 2B.[39] The is because the template generated a different environment in the MIP being modified in relation to the NIP by the impression of active selective sites.

The morphology and structures of the MIPs, unextracted MIPs and NIPs were characterized by SEM. According to the SEM images, MIPs and unextracted MIPs display a agglomerated, concrete-like shape and visible chromatism with similar sizes, as observed in Fig. 3A and B. Before extraction, the shape of MIPs is not very clear probably due to the influence of other remainders.[40] The shape of MIPs becomes more smooth, discernible through the elution process. However, the NIPs (Fig. 3C) exhibit heterogeneous and irregular morphology, which means that the absence of the template molecule could be involved in the synthesis of the polymer to some extent.[41] These results are also in agreement with the finding that additional molecular interaction occurs between template and MAA, which could somehow help the growth of the cross-linked polymer nuclei to result in a more regular polymer structure in solutions.[42]
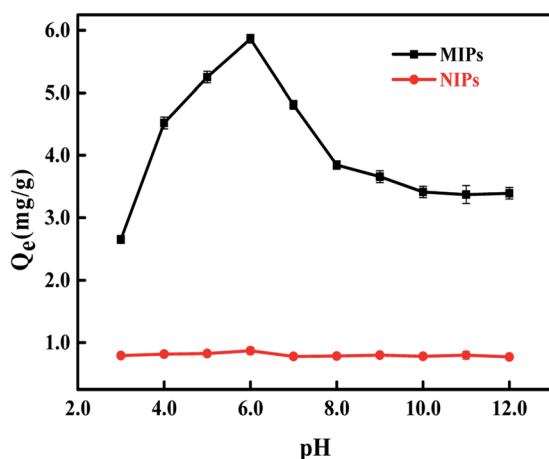
3.3 Effect of pH

To achieve the maximum adsorption capacity, the influence of different pH values of PBS solutions was investigated, and the result is displayed in Fig. 4. The result shows that the adsorption capacity of MIPs increased from pH 3.0 to 6.0 and reached the maximum adsorption capacity at pH 6.0, which agrees with the basic characteristic of cathinones. At pH 6.0, 4-MDMC becomes positively charged due to the protonation of the amine moieties, resulting in effective interactions with the MIP cavities via electrostatic interactions.[43,44] However, with the further increase in pH, there is a gradual decrease observed in the adsorption capacity, mainly attributing to the restriction of the electrostatic attraction forces between 4-MDMC and MIPs.[45,46] The pK_a value of 4-MDMC is 7.09. Instead, there is not a distinct effect of different pH conditions on adsorption capacity of NIPs. An optimal pH of 6.0 was chosen as the further adsorption experiments.

3.4 Adsorption isotherms

To demonstrate the rebinding features of the MIPs and NIPs, the isothermal adsorption experiments were explored with the 4-MDMC initial concentration range from 5 mg L^{-1} to 50 mg L^{-1} at 298 K, 308 K and 318 K respectively. The variation in the adsorption equilibrium capacity (Q_e) with initial concentration is displayed in Fig. 5A. It can be clearly observed that with the increase in 4-MDMC initial concentration, the adsorption capacity of MIPs for 4-MDMC increased. While NIPs display a little dependence on the concentration and lower adsorption amounts due to lack of recognition sites. Besides, with the increment in temperature, the Q_e value of 4-MDMC shows the same trend and gets enhanced, indicating that MIPs have more satisfactory efficiency at higher temperatures. As a result, the high imprinting factor (α) was 8.45 at 308 K, suggesting the MIPs possessed excellent selectivity for template molecule 4-MDMC, because a large number of binding sites were existent.

The Langmuir (eqn (7)), Freundlich (eqn (8)), Temkin (eqn (9)) and Slips or Langmuir–Freundlich (in ESI†) isotherm adsorption models were employed to assess the isotherm binding mechanism:

$$\frac{C_e}{Q_e} = \frac{1}{Q_m K_L} + \frac{C_e}{Q_m} \quad (7)$$

$$\log Q_e = \frac{1}{n} \log C_e + \log K_f \quad (8)$$

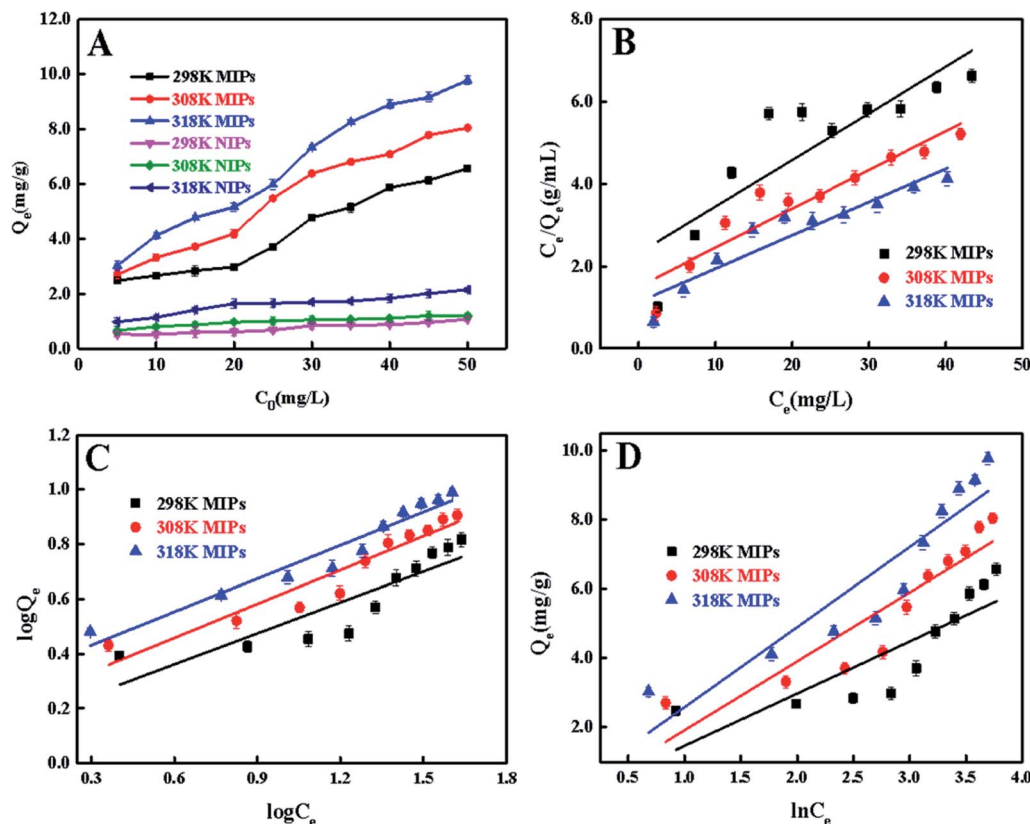$$Q_e = B \ln A + B \ln C_e \quad (9)$$

Fig. 4 Effect of pH on the adsorption capacity of MIPs and NIPs to 4-MDMC.

Fig. 5 (A) Static adsorption isotherms of 4-MDMC onto MIPs and NIPs at different temperatures; (B) Langmuir adsorption model, (C) Freundlich adsorption model, and (D) Temkin adsorption model of 4-MDMC onto MIPs at different temperatures.

where C_e (mg mL^{-1}) is the concentration of 4-MDMC at adsorption equilibrium, Q_e (mg g^{-1}) is the amount of the analyte adsorbed at equilibrium, and Q_m (mg g^{-1}) is the theoretical maximum adsorption capacity. K_L (mL g^{-1}) and K_F (mg g^{-1}) represent Langmuir and Freundlich constants, respectively. n is the heterogeneity factor. B is related to the heat of adsorption and A refers to the dimensionless Temkin isotherm constant. The linear fitting curves of MIPs and NIPs at different temperatures based on Langmuir, Freundlich, Temkin and Slips or Langmuir–Freundlich isotherm models are illustrated in Fig. 5B, C, D, S2 and S3,† respectively. In addition, the relevant fitting parameters are meanwhile detailed in the ESI (Table S1†). It can be seen that the adsorption process is more suitable by the Slips or Langmuir–Freundlich model than Langmuir, Freundlich and Temkin. In general, the Freundlich isotherm model demonstrates that the monolayer single-solute adsorption from dilute solutions on heterogeneous solid surfaces show quasi-Gaussian distribution of adsorption energies.[47,48] Besides, the related parameters of MIPs to 4-MDMC at different temperatures are better than those of NIPs, which also suggest an excellent imprinting effect owing to the presence of a large number of selective binding sites on the MIPs.

3.5 Adsorption kinetics

The extended binding kinetics of 4-MDMC onto MIPs and NIPs at different temperatures were carried out to evaluate the adsorption efficiency. From Fig. 6A, it can be observed that the adsorption capacity of 4-MDMC onto MIPs increased rapidly in the beginning 30 min and gradually slowed down till equilibrium. For NIPs, it has a similar trend but displays a lower adsorption capacity. The differences in the adsorption capacity can be explained as follows: the MIPs can obtain a large amount of empty recognition sites through the exhaustive washing procedure, which are matched well with the template molecules in size, shape and chemical functionality. However, functional monomers belong to a state of disorder in NIPs, which could be unable to formulate tailored imprinting cavities. Therefore, it results in non-specific adsorption between NIPs and 4-MDMC only by van der Waals force procedure. With the extension of reaction time, the adsorption tends to be saturated showing a slight increase, possibly indicating that most of the recognition sites were occupied by 4-MDMC.[49] According to previous reports and results in this study, the adsorption of 4-MDMC is a spontaneous and strong endothermic process.[50,51] With the increment in temperature, the thermal movements of the 4-MDMC in solution are favored, resulting in a higher adsorption capacity and a fast mass transfer. The pseudo-first-order and pseudo-second-order models (Fig. S4† and 6B–D) were further applied for fitting analysis according to the following equations, and the relevant fitting parameters are illustrated in the ESI (Table S2†).
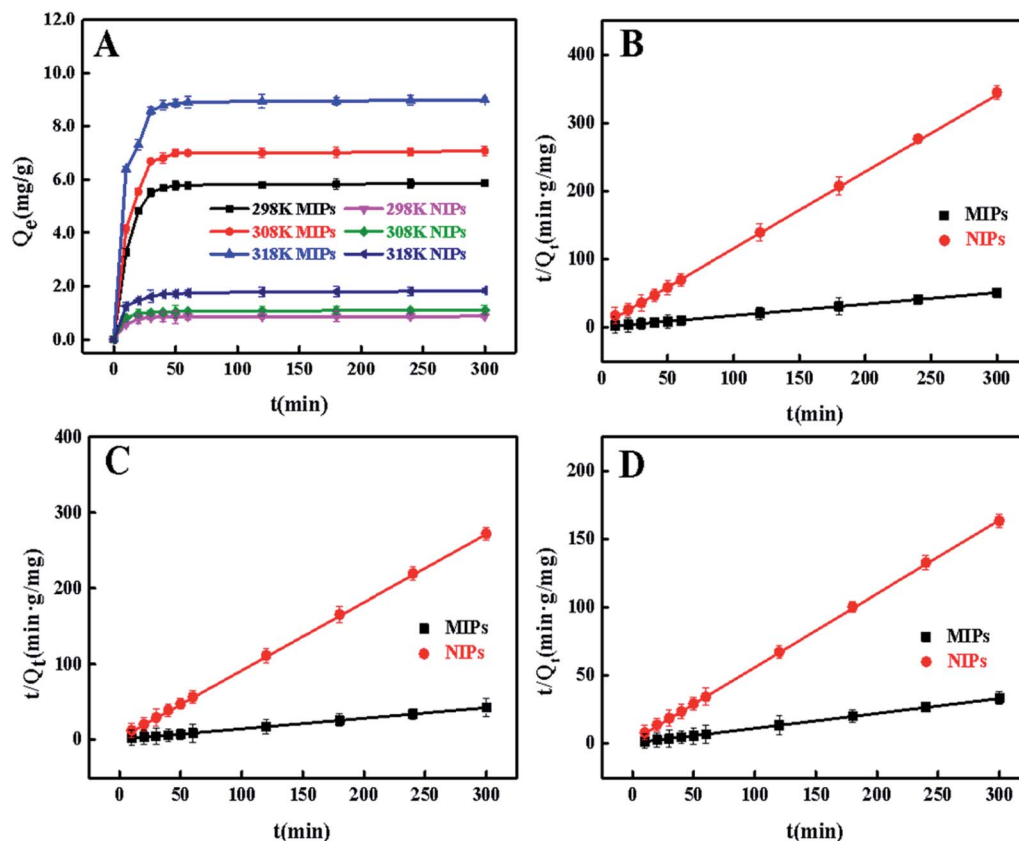
Fig. 6 Adsorption kinetics of 4-MDMC onto MIPs and NIPs at different temperatures (A). Pseudo-second-order model of 4-MDMC onto MIPs and NIPs at 298 K (B). 308 K (C). 318 K (D).

$$\log(Q_e - Q_t) = \log Q_e - \frac{K_1 t}{2.303} \quad (10)$$

$$\frac{t}{Q_t} = \frac{1}{K_2 Q_e^2} + \frac{t}{Q_e} \quad (11)$$

where Q_e (mg g^{-1}) and Q_t (mg g^{-1}) are the adsorption amounts of the template and analogues on MIPs (or NIPs), respectively.

3.6 Selectivity and reusability analysis

To investigate the selective recognition of the MIPs prepared in this method, 4-EMC, βk-MBDP, MXE and THF-F were selected as the competitive compounds at 308 K, as demonstrated in Fig. 7A. As observed, MIPs exhibit a higher adsorption capacity for 4-MDMC, and the selectivity coefficients of 4-EMC, βk-MBDP, MXE and THF-F are 1.70, 3.49, 7.14 and 5.82 respectively, while the bound amounts of the NIPs show poor selectivity to all. The pK_a values of 4-EMC, βk-MBDP, MXE and THF-F
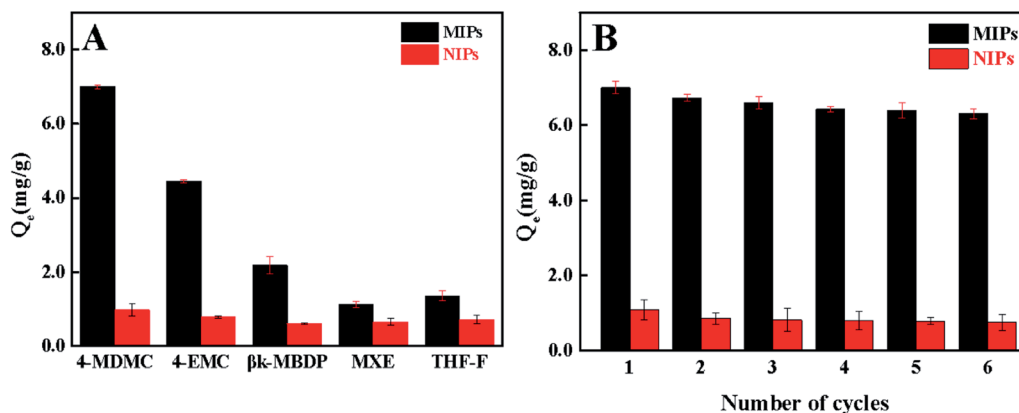

Fig. 7 (A) Binding selectivity of MIPs and NIPs for 4-MDMC and its competitive compounds in pH = 6.0 PBS solution. (B) Regeneration of MIPs and recoveries for 4-MDMC in six successive cycles of adsorption–desorption.

are 7.38, 7.74, 7.40 and 7.76, respectively. This results in the existence of recognition cavity, which is closely related to the similarity between the template and the adsorbed molecules in functional groups, size and shape.[52] At the same time, the binding capacity of MIPs on 4-EMC is higher than that of the other three compounds due to the similar structure to 4-MDMC.

Besides, MIPs and NIPs were subjected to six cycles of adsorption–desorption for 4-MDMC at 308 K to test the reusability and stability of the adsorbents. As shown in Fig. 7B, the adsorption capacity of the regenerated MIPs is about 9.94% loss after six consecutive adsorption–desorption cycles, indicating that the synthesized MIPs have good mechanical stability and could be reused repeatedly with only a slight decrease in the adsorption capacity. The results also demonstrate that the MIPs provide more stable recognition sites in imprinting polymer materials.

3.7 Analysis of 4-MDMC in human urine

To evaluate the practical applicability of the prepared MIPs, it was applied to the sorption and removal of 4-MDMC from human urine samples, followed by HPLC determination. After the treatment described above, no 4-MDMC at detectable levels were found in the urine obtained from a healthy volunteer. Then, the urine samples were spiked with 4-MDMC at three spiked levels of 40, 200 and 400 $\mu g\ L^{-1}$, respectively. After the same treatment procedures, the recoveries of 4-MDMC in three urine samples were found to be 69.3, 75.5, and 78.9%, respectively (in Table S3†), demonstrating the potential capability of MIPs for separating 4-MDMC from urine samples.

4. Conclusion

In summary, MIPs have been successfully synthesized by a simple non-covalent polymerization process and the relevant adsorption experiments were studied. The advantage of this whole procedure is simple and economic in operation, and mild in reaction conditions. It was found from adsorption experiments that the adsorption was a spontaneous and endothermic process, and the MIPs exhibited short adsorption equilibrium time, excellent recognition performance, high adsorption efficiency, and good reusability. Based on comparison with NIPs, it can be shown that MIPs possessed both selective and nonselective binding sites, whereas NIPs can only be absorbed by van der Waals force. Satisfactory recoveries in spiked human urine proved the potential of MIPs in the rapid and selective removal of 4-MDMC. Hence, all the results indicated that the MIPs could be expected to be used as promising materials for the selective removal of 4-MDMC from complicated solutions.

Conflicts of interest

There are no conflicts to declare.

Acknowledgements

References

1 W. W. Y. Lee, V. A. D. Silverson, L. E. Jones, Y. C. Ho, N. C. Fletcher, M. McNaul, K. L. Peters, S. J. Speers and S. E. J. Bell, Surface-enhanced Raman spectroscopy of novel psychoactive substances using polymer-stabilized Ag nanoparticle aggregates, *Chem. Commun.*, 2016, **52**, 493–496.

2 D. Rouxinol, H. Carmo, F. Carvalho, M. D. L. Bastos and D. D. da Silva, Pharmacokinetics, pharmacodynamics, and toxicity of the new psychoactive substance 3,4-dimethylmethcathinone (3,4-DMMC), *Forensic Toxicol.*, 2020, **38**, 15–29.

3 D. M. Calinski, D. F. Kisor and J. E. Sprague, A review of the influence of functional group modifications to the core scaffold of synthetic cathinones on drug pharmacokinetics, *Psychopharmacology*, 2019, **236**, 881–890.

4 M. J. Valente, P. G. de Pinho, M. d. L. Bastos, F. Carvalho and M. Carvalho, Khat and synthetic cathinones: a review, *Arch. Toxicol.*, 2014, **88**, 15–45.

5 K. Miotto, J. Striebel, A. K. Cho and C. Wang, Clinical and pharmacological aspects of bath salt use: A review of the literature and case reports, *Drug Alcohol Depend.*, 2013, **132**, 1–12.

6 W.-C. Cheng and W.-C. Wong, Forensic drug analysis of chloro-N, N-dimethylcathinone (CDC) and chloroethcathinone (CEC): Identification of 4-CDC and 4-CEC in drug seizures and differentiation from their ring-substituted positional isomers, *Forensic Sci. Int.*, 2019, **298**, 268–277.

7 A. L. Riley, K. H. Nelson, P. To, R. Lopez-Arnau, P. Xu, D. Wang, Y. Wang, H.-w. Shen, D. M. Kuhn, M. Angoa-Perez, J. H. Anneken, D. Muskiewicz and F. S. Hall, Abuse potential and toxicity of the synthetic cathinones (i.e., "Bath salts"), *Neurosci. Biobehav. Rev.*, 2020, **110**, 150–173.

8 L. H. Antonides, R. M. Brignall, A. Costello, J. Ellison, S. E. Firth, N. Gilbert, B. J. Groom, S. J. Hudson, M. C. Hulme, J. Marron, Z. A. Pullen, T. B. R. Robertson, C. J. Schofield, D. C. Williamson, E. K. Kemsley, O. B. Sutcliffe and R. E. Mewis, Rapid Identification of Novel Psychoactive and Other Controlled Substances Using Low-Field(1)H NMR Spectroscopy, *ACS Omega*, 2019, **4**, 7103–7112.

9 S. S. Rossi, S. Odoardi, A. Gregori, G. Peluso, L. Ripani, G. Ortar, G. Serpelloni and F. S. Romolo, An analytical approach to the forensic identification of different classes of new psychoactive substances (NPSs) in seized materials, *Rapid Commun. Mass Spectrom.*, 2014, **28**, 1904–1916.

10 M. Majchrzak, R. Celinski, P. Kus, T. Kowalska and M. Sajewicz, The newest cathinone derivatives as designer

drugs: an analytical and toxicological review, *Forensic Toxicol.*, 2018, **36**, 33–50.

11 A. D. Lesiak, R. A. Musah, R. B. Cody, M. A. Domin, A. J. Dane and J. R. E. Shepard, Direct analysis in real time mass spectrometry (DART-MS) of "bath salt" cathinone drug mixtures, *Analyst*, 2013, **138**, 3424–3432.

12 S. Mabbott, A. Eckmann, C. Casiraghi and R. Goodacre, 2p or not 2p: tuppence-based SERS for the detection of illicit materials, *Analyst*, 2013, **138**, 118–122.

13 J. P. Metters, M. Gomez-Mingot, J. Iniesta, R. O. Kadara and C. E. Banks, The fabrication of novel screen printed single-walled carbon nanotube electrodes: Electroanalytical applications, *Sens. Actuators, B*, 2013, **177**, 1043–1052.

14 J. P. Smith, O. B. Sutcliffe and C. E. Banks, An overview of recent developments in the analytical detection of new psychoactive substances (NPSs), *Analyst*, 2015, **140**, 4932–4948.

15 Y. Hoshino, H. Koide, T. Urakami, H. Kanazawa, T. Kodama, N. Oku and K. J. Shea, Recognition, Neutralization, and Clearance of Target Peptides in the Bloodstream of Living Mice by Molecularly Imprinted Polymer Nanoparticles: A Plastic Antibody, *J. Am. Chem. Soc.*, 2010, **132**, 6644–6645.

16 L. Chen, S. Xu and J. Li, Recent advances in molecular imprinting technology: current status, challenges and highlighted applications, *Chem. Soc. Rev.*, 2011, **40**, 2922–2942.

17 S. Chunta, R. Suedee, W. Boonsriwong and P. A. Lieberzeit, Biomimetic sensors targeting oxidized-low-density lipoprotein with molecularly imprinted polymers, *Anal. Chim. Acta*, 2020, **1116**, 27–35.

18 M. Bilici, A. Zengin, E. Ekmen, D. Cetin and N. Aktas, Efficient and selective separation of metronidazole from human serum by using molecularly imprinted magnetic nanoparticles, *J. Sep. Sci.*, 2018, **41**, 2952–2960.

19 S. Nasirahmadi and J. Zargan, Research Paper: Bioinformatics Analysis of Linear B-cell Viscumin Toxin Epitope With Potential Use in Molecularly Imprinted Polymer Biosensors, *Int. J. Med. Toxicol. Forensic Med.*, 2020, **10**, 26172–26179.

20 W. Xu, X. Zhang, W. Huang, Y. Luan, Y. Yang, M. Zhu and W. Yang, Synthesis of surface molecular imprinted polymers based on carboxyl-modified silica nanoparticles with the selective detection of dibutyl phthalate from tap water samples, *Appl. Surf. Sci.*, 2017, **426**, 1075–1083.

21 A. Molinelli, R. Weiss and B. Mizaikoff, Advanced solid phase extraction using molecularly imprinted polymers for the determination of quercetin in red wine, *J. Agric. Food Chem.*, 2002, **50**, 1804–1808.

22 L. L. Zhu and X. J. Xu, Selective separation of active inhibitors of epidermal growth factor receptor from Caragana Jubata by molecularly imprinted solid-phase extraction, *J. Chromatogr. A*, 2003, **991**, 151–158.

23 S. A. Nabavi, G. T. Vladisavljevic, A. Wicaksono, S. Georgiadou and V. Manovic, Production of molecularly imprinted polymer particles with amide-decorated cavities for CO_2 capture using membrane emulsification/

suspension polymerisation, *Colloids Surf., A*, 2017, **521**, 231–238.

24 X. Wang, P. Huang, X. Ma, X. Du and X. Lu, Magnetic mesoporous molecularly imprinted polymers based on surface precipitation polymerization for selective enrichment of triclosan and triclocarban, *J. Chromatogr. A*, 2018, **1537**, 35–42.

25 T. A. Sergeyeva, O. A. Slinchenko, L. A. Gorbach, V. F. Matyushov, O. O. Brovko, S. A. Piletsky, L. M. Sergeeva and G. V. Elska, Catalytic molecularly imprinted polymer membranes: Development of the biomimetic sensor for phenols detection, *Anal. Chim. Acta*, 2010, **659**, 274–279.

26 J. Javidi, M. Esmaeilpour and M. R. Khansari, Synthesis, characterization and application of core-shell magnetic molecularly imprinted polymers for selective recognition of clozapine from human serum, *RSC Adv.*, 2015, **5**, 73268–73278.

27 P. S. Sharma, A. Pietrzyk-Le, F. D'Souza and W. Kutner, Electrochemically synthesized polymers in molecular imprinting for chemical sensing, *Anal. Bioanal. Chem.*, 2012, **402**, 3177–3204.

28 B. C. Cui, P. Liu, X. J. Liu, S. Z. Liu and Z. H Zhang, Molecularly imprinted polymers for electrochemical detection and analysis: progress and perspectives, *J. Mater. Res. Technol.*, 2020, **9**(xx), 12568–12584.

29 F. Tan, D. Sun, J. Gao, Q. Zhao, X. Wang, F. Teng, X. Quan and J. Chen, Preparation of molecularly imprinted polymer nanoparticles for selective removal of fluoroquinolone antibiotics in aqueous solution, *J. Hazard. Mater.*, 2013, **244**, 750–757.

30 H. Liu, L. Ding, L. Chen, Y. Chen, T. Zhou, H. Li, Y. Xu, L. Zhao and N. Huang, A facile, green synthesis of biomass carbon dots coupled with molecularly imprinted polymers for highly selective detection of oxytetracycline, *J. Ind. Eng. Chem.*, 2019, **69**, 455–463.

31 I. Vasconcelos, P. H. Reis da Silva, D. R. Davila Dias, M. B. de Freitas Marques, W. d. N. Mussel, T. A. Pedrosa, M. E. S. Ribeiro e Silva, R. F. de Souza Freitas, R. G. de Sousa and C. Fernandes, Synthesis and characterization of a molecularly imprinted polymer (MIP) for solid-phase extraction of the antidiabetic gliclazide from human plasma, *Mater. Sci. Eng., C*, 2020, **116**, 111191.

32 L. Filipe-Ribeiro, F. Cosme and F. M. Nunes, New molecularly imprinted polymers for reducing negative volatile phenols in red wine with low impact on wine colour, *Food Res. Int.*, 2020, **129**, 108855.

33 Y. Xiao, R. Xiao, J. Tang, Q. Zhu, X. Li, Y. Xiong and X. Wu, Preparation and adsorption properties of molecularly imprinted polymer via RAFT precipitation polymerization for selective removal of aristolochic acid I, *Talanta*, 2017, **162**, 415–422.

34 J. Bai, Y. Zhang, W. Zhang, X. Ma, Y. Zhu, X. Zhao and Y. Fu, Synthesis and characterization of molecularly imprinted polymer microspheres functionalized with POSS, *Appl. Surf. Sci.*, 2020, **511**, 145506–145516.

35 H.-W. Chien, M.-T. Tsai, C.-H. Yang, R.-H. Lee and T.-L. Wang, Interaction of LiYF$_4$:Yb^{3+}/Er^{3+}/Ho^{3+}/Tm^{3+}@LiYF$_4$:Yb($^{3+}$) upconversion nanoparticles, molecularly imprinted polymers, and templates, *RSC Adv.*, 2020, **10**, 35600–35610.

36 S. Wang, Y. Geng, X. Sun, R. Wang, Z. Zheng, S. Hou, X. Wang and W. Ji, Molecularly imprinted polymers prepared from a single cross-linking functional monomer for solid-phase microextraction of estrogens from milk, *J. Chromatogr. A*, 2020, **1627**, 461400.

37 S. Farzaneh, E. Asadi, M. Abdouss, A. Barghi-Lish, S. Azodi-Deilami, H. A. Khonakdar and M. Gharghabi, Molecularly imprinted polymer nanoparticles for olanzapine recognition: application for solid phase extraction and sustained release, *RSC Adv.*, 2015, **5**, 9154–9166.

38 D. M. Sartore, D. A. Vargas Medina, J. L. Costa, F. M. Lancas and A. J. Santos-Neto, Automated microextraction by packed sorbent of cannabinoids from human urine using a lab-made device packed with molecularly imprinted polymer, *Talanta*, 2020, **219**, 121185.

39 Y. Xia, F. Zhao and B. Zeng, A molecularly imprinted copolymer based electrochemical sensor for the highly sensitive detection of L-Tryptophan, *Talanta*, 2020, **206**, 120245.

40 D. Wang, X. Luo, M. Wang, K. Zhou and Z. Xia, Selective separation and purification of polydatin by molecularly imprinted polymers from the extract of Polygoni Cuspidati Rhizoma et Radix, rats' plasma and urine, *J. Chromatogr. B: Anal. Technol. Biomed. Life Sci.*, 2020, **1156**, 122307.

41 K. Yoshimatsu, K. Reimhult, A. Krozer, K. Mosbach, K. Sode and L. Ye, Uniform molecularly imprinted microspheres and nanoparticles prepared by precipitation polymerization: The control of particle size suitable for different analytical applications, *Anal. Chim. Acta*, 2007, **584**, 112–121.

42 H. Zeng, X. Yu, J. Wan and X. Cao, Rational design and synthesis of molecularly imprinted polymers (MIP) for purifying tylosin by seeded precipitation polymerization, *Process Biochem.*, 2020, **94**, 329–339.

43 J. Sanchez-Gonzalez, S. Odoardi, A. Maria Bermejo, P. Bermejo-Barrera, F. Saverio Romolo, A. Moreda-Pineiro and S. Strano-Rossi, HPLC-MS/MS combined with membrane-protected molecularly imprinted polymer micro-solid-phase extraction for synthetic cathinones monitoring in urine, *Drug Test. Anal.*, 2019, **11**, 33–44.

44 T. Murakami, Y. Iwamuro, R. Ishimaru, S. Chinaka and H. Hasegawa, Molecularly imprinted polymer solid-phase extraction of synthetic cathinones from urine and whole blood samples, *J. Sep. Sci.*, 2018, **41**, 4506–4514.

45 Z. Liu, Y. Wang, F. Xu, X. Wei, J. Chen, H. Li, X. He and Y. Zhou, A new magnetic molecularly imprinted polymer based on deep eutectic solvents as functional monomer and cross-linker for specific recognition of bovine hemoglobin, *Anal. Chim. Acta*, 2020, **1129**, 49–59.

46 G. Z. Kyzas, S. G. Nanaki, A. Koltsakidou, M. Papageorgiou, M. Kechagia, D. N. Bikiaris and D. A. Lambropoulou, Effectively designed molecularly imprinted polymers for selective isolation of the antidiabetic drug metformin and its transformation product guanylurea from aqueous media, *Anal. Chim. Acta*, 2015, **866**, 27–40.

47 I. Jaroniec, A. Deryto and A. Marczewski, The Langmuir-Freundlich equation in adsorption from dilute solutions on solids, *Monatsh. Chem.*, 1983, **114**, 393–397.

48 R. J. Umpleby, S. C. Baxter, Y. Z. Chen, R. N. Shah and K. D. Shimizu, Characterization of molecularly imprinted polymers with the Langmuir-Freundlich isotherm, *Anal. Chem.*, 2001, **73**, 4584–4591.

49 S. Hosseini, M. A. Khan, M. R. Malekbala, W. Cheah and T. S. Y. Choong, Carbon coated monolith, a mesoporous material for the removal of methyl orange from aqueous phase: Adsorption and desorption studies, *Chem. Eng. J.*, 2011, **171**, 1124–1131.

50 Q. Wu, M. Li, Z. Huang, Y. Shao, L. Bai and L. Zhou, Well-defined nanostructured core-shell magnetic surface imprinted polymers (Fe$_3$O$_4$@SiO$_2$@MIPs) for effective extraction of trace tetrabromobisphenol A from water, *J. Ind. Eng. Chem.*, 2018, **60**, 268–278.

51 X. Li, X. Ma, R. Huang, X. Xie, L. Guo and M. Zhang, Synthesis of a molecularly imprinted polymer on mSiO$_2$@Fe$_3$O$_4$ for the selective adsorption of atrazine, *J. Sep. Sci.*, 2018, **41**, 2837–2845.

52 H. Li, M. Xu, S. Wang, C. Lu and Z. Li, Preparation, characterization and selective recognition for vanillic acid imprinted mesoporous silica polymers, *Appl. Surf. Sci.*, 2015, **328**, 649–657.